AIP Journal of Applied Physics

Iron oxide nanoparticles coated with gold: Enhanced magnetic moment due to interfacial effects

S. Banerjee, S. O. Raja, M. Sardar, N. Gayathri, B. Ghosh, and A. Dasgupta

Citation: Journal of Applied Physics **109**, 123902 (2011); doi: 10.1063/1.3596760
View online: http://dx.doi.org/10.1063/1.3596760
View Table of Contents: http://scitation.aip.org/content/aip/journal/jap/109/12?ver=pdfcov
Published by the AIP Publishing

Iron oxide nanoparticles coated with gold: Enhanced magnetic moment due to interfacial effects

S. Banerjee,[1,a)] S. O. Raja,[2] M. Sardar,[3] N. Gayathri,[4] B. Ghosh,[1] and A. Dasgupta[2]
[1]*Surface Physics Division, Saha Insitute of Nuclear Physics, 1/AF Bidhannagar, Kolkata 700 064, India*
[2]*Department of Biochemistry, University of Calcutta, 35 B. C. Road, Kolkata-700019, India*
[3]*Material Science Division, Indira Gandhi Center for Atomic Research, Kalpakkam 603 102, India*
[4]*Material Science Section, Variable Energy Cyclotron Center, 1/AF Bidhannagar, Kolkata 700 064, India*

(Received 6 February 2011; accepted 2 May 2011; published online 17 June 2011)

In this paper, we show that when nanoparticles of Fe_3O_4 are coated with gold there is a distinct enhancement of magnetization by a factor of six. This increase of magnetization has been attributed to large orbital magnetic moment formation at the magnetic particle/Au (core/shell) interface. Our theoretical analysis indicates that the enhanced magnetism observed in Fe_3O_4-Au (core-shell) nanoparticles is an interfacial effect. The origin of magnetism in Au as an interfacial phenomenon is supported by the observation of positive magnetization in citrate coated gold nanoparticles. In citrate coated gold nanoparticles, we observe a crossover from positive magnetization value to negative magnetization value upon increasing magnetic field indicating cancellation of interfacial magnetization by the diamagnetic contribution from the bulk. We propose a theoretical formalism which semi-quantitatively explains our experimental results and supports the origin of magnetization in Au as an interfacial effect. © *2011 American Institute of Physics*. [doi:10.1063/1.3596760]

I. INTRODUCTION

Magnetism in nano/colloidal particles has become a subject of intense research interest in recent years.[1–3] Their rich contribution to fundamental physics and their importance in technological application has become well established now.[4] The observation of decrease in diamagnetic susceptibility of copper, silver, gold and even antimony, bismuth, and graphite on colloidalization has been a puzzle since long ago [see the series of papers published in 1920s and 1930s (Ref. 5)]. Now we believe that we understand the appearance of magnetism in these type of systems as not due to the atomic spins but due to the orbital moments occurring at the defect sites as we have pointed out in the case of ZnO.[6]

Multicomponent nanoparticles (NP) shows many interesting magnetic,[7] optical,[8] and catalytic[9] properties. Core-shell NPs, with magnetic materials (metallic or insulating) as core and nonmagnetic (metallic or insulating) materials as shell, are an active field of research to achieve multifunctionality in a single material. Au coated Fe_3O_4 NPs are an attractive system[10,11] that might have interesting magnetic and optical properties and important biomedical applications because of negligible cytotoxicity of Au.

In a parallel development over the last decade, ferromagnetism in graphite,[12] nonmagnetic oxides and borides[6,13,14] have been reported and the ferromagnetic hysteresis observed in these systems have also been attributed to orbital magnetism[6,15] occurring due to nanosize defects/structures. Polymer stabilized metallic NPs like Au and Pd were found to be magnetic.[16] Thiol capped Au nanoparticles[17–19] and even bare Pd, Au clusters made by gas evaporation method were also found to possess finite magnetic moments.[20] It has also been observed that when Fe_3O_4 is coated with Al (Fe_3O_4/Al bilayer) there is enhancement of magnetization.[21] All the above observations may indicate that there may be a common origin for the observation of magnetization or its enhancement and it may be due to the presence of an interface. This additional magnetization can arise due to an interfacial effect.

In this paper, we have carried out a systematic study to understand the role of gold in modifying the magnetization of Fe_3O_4 NPs upon incorporation of Au NPs. We have observed that when Au-NPs covers Fe_3O_4 NPs resulting in a core-shell structure, the magnetism enhances drastically. In this paper, we report the synthesis, structure, and magnetic characterization of composites of cluster of Fe_3O_4 NPs coated with Au NPs. The results could be modeled by attributing the magnetism as arising due to the interfacial effect between the Au NPs shell and the core of the aggregated Fe_3O_4 NPs. To give a supporting evidence on this interfacial effect, we have compared the results obtained with that of Au-NPs coated with citrate which establishes that indeed the magnetism observed in these composite systems is arising due to the interfacial effect between the Au and the other component which may be either magnetic or non-magnetic. Observation of magnetism in a pure gold system can always raise doubt about the unintentional impurity introduced during sample preparation and handling but for the Fe_3O_4-Au system we have intentionally incorporated magnetic impurity (Fe_3O_4) and have shown that in certain structural condition indeed the magnetization increases (the interfacial contribution).

II. EXPERIMENTAL

Fe_3O_4 NPs were initially prepared by co-precipitation method. Four gm ferric chloride and 2 gm ferrous chloride

[a)]Electronic mail: sangam.banerjee@saha.ac.in. See also arXiv:0906.1497v2 for more data on magnetic property.

(2:1, w/w ratio) were dissolved in 2 M HCl and co-precipitated by 100 ml 1.5 M NaOH solution upon constant stirring for 30 mins at room temperature. The prepared colloidal solution was centrifuged to collect the supernatant (suspended) solution to obtain particles with a narrow size distribution. The supernatant solution was pelleted down by a strong magnet and washed four times by ultra pure water. Finally, 20 ml Citrate buffer (1.6 gm citric acid and 0.8 gm tri-sodium citrate) was added to collect the stabilized ferrofluid in solution at a pH around 6.3. This solution was used as a base in the subsequent preparation of the nanocomposite samples. The solution was lyophilized to obtain the pure Fe_3O_4 sample which will be referred to subsequently as Sample A. The following procedure was adopted to prepare the Au:Fe_3O_4 nanocomposite samples: 300 μL of the synthesized colloidal iron oxide nanoparticle (0.1 M) suspension was added to 25 ml ultra pure boiling water under vigorous stirring condition. Then 350 μL of 20 mM $HAuCl_4$ is added and finally 300 μL of 100 mM tri-sodium citrate was added. The whole solution was kept boiling and stirred for 15 mins till the color of the solution turned from black to red. The TEM measurement on this sample revealed polydispersed nanoparticles with 5–10 nm size along with very large particles (~200 nm in size) having core-shell structures with Fe_3O_4 at the core and Au as the outer shell growth driven by coalescence process.[22] To separate out these large particles, the red solution was further centrifuged. In Fig. 1 we show the TEM micrograph of the (a) supernatant and (b–d) pellet solutions. The particles appearing with lower contrast are Fe_3O_4 particles and those with high contrast (dark) are the Au particles. In both the samples, the Fe_3O_4 particles are typically 3–4 nm in size. The Au particles in the supernatant sample are nearly monodispered with particle size ~5–6 nm whereas in the pellet sample, they are polydispersed with the particle sizes ranging from ~7–10 nm. In the low magnification micrographs Fig. 1(c–d) of the pellet sample, we could now easily observe the very large particles (~200 nm in size) having core-shell structures with Fe_3O_4 at the core and Au as the outer shell. These large core-shell particles were not observed in the supernatant sample. The supernatant and the pellet solutions were lyophilized to obtain the dry supernatant sample (Sample B) and the pellet sample (Sample C), respectively. This resulted in two samples with different Au NPs sizes keeping the Fe_3O_4 particle size same. We would like to mention here that the concentration of the auric chloride taken for our sample preparation seems to be a critical concentration for obtaining these large core-shell particles. We could not obtain these large particles either with a lower or higher concentration of auric chloride. The Atomic Absorption Spectroscopic (Varian AA240) analysis was performed to measure the iron and gold content in the supernatant and in the pellet. The particles were digested in aqua regia (HCl: HNO3 = 3:1) to prepare the samples. The standards were 1, 5, 10, and 25 mg/L for both (iron and gold). Aqua regia in same proportion was used as a blank to avoid the iron contribution from HCl and water. In the supernatant the Au and Fe content were found to be 0.46 mg/L and 3.789 mg/L, respectively. Hence, percentage of gold was 10.82% in the supernatant sample. In the pellet sample the Au and Fe content were found to be 5.132 mg/L and 12.749 mg/L, respectively, giving a percentage of gold to be 28.7%. TEM images and the corresponding electron diffraction obtained from Fe_3O_4 particles and the core of the high Au content core-shell particles are shown in Fig. 2. The electron diffraction rings obtained from the samples could be indexed to that of Fe_3O_4. In Fig. 2(d) we can see that there is a clear signature of Fe_3O_4 from the core of the Au-Fe_3O_4 core-shell structure. The density of Fe_3O_4 is much lower than that of Au and hence we observe more transmission through the center of the particle indicating that the core region is mainly Fe_3O_4. The Au-NPs coated with citrate were prepared by a similar procedure. 350 μL 20 mM auric chloride ($HAuCl_3$) solution is added to boiling 25 ml milli-Q water under vigorous stirring. Then 100 mM 300 μL tri-sodium citrate is added. After

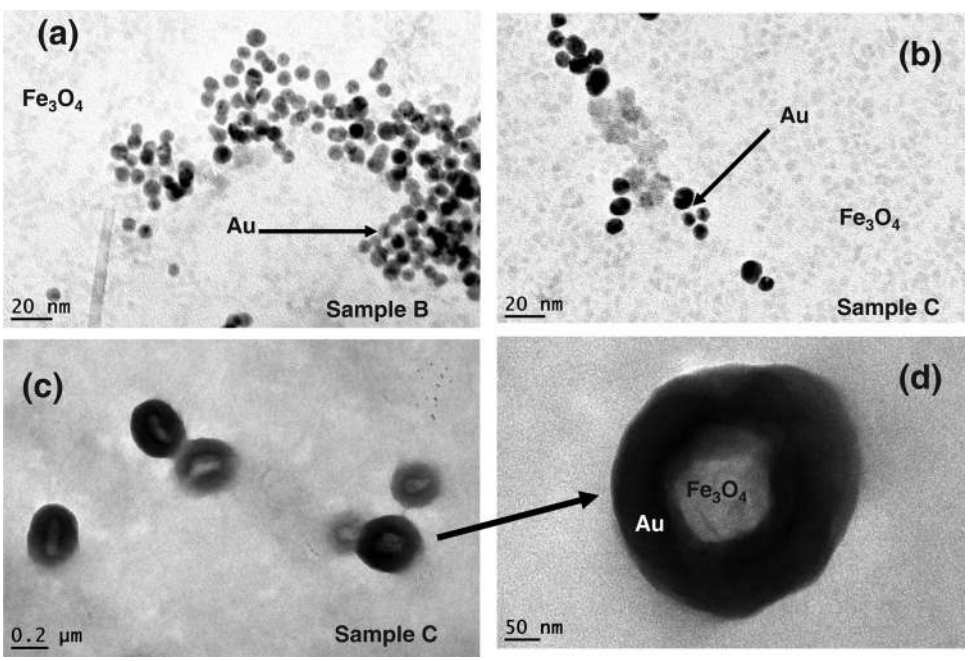

FIG. 1. (See online for better contrast of Fe_3O_4 particles.) Transmission electron micrographs of the (a) Sample B (Low-Au) and (b-d) Sample C (High-Au) nanocomposites. Fe_3O_4 can be seen in the background as faint particles of size 3–4 nm. Au particles are darker and are marked by arrows. Core(Fe_3O_4)-shell(Au) structures seen in Sample C are shown in (c) and (d).

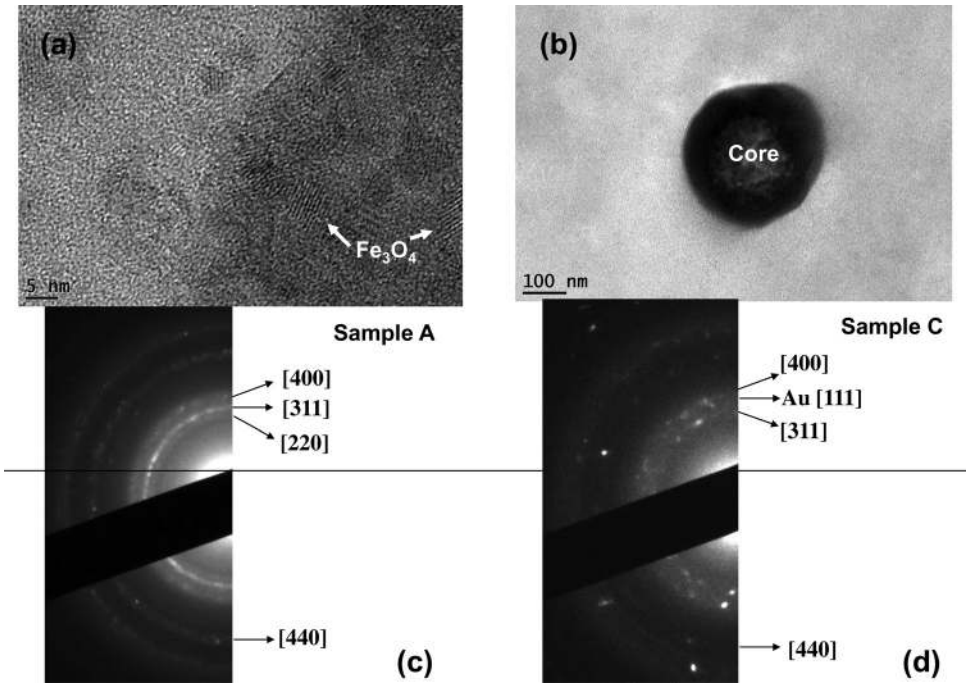

FIG. 2. Transmission electron micrographs and electron diffraction: (a) and (c) Sample A (Fe_3O_4); (b) and (d) core of the Sample C core shell particles. The diffraction rings in the (d) clearly shows presence of Fe_3O_4.

sometime (4 mins) a blue color appears. This color changes to pink then to light red and finally to deep red. The solution is allowed to stand for another 15 mins after the appearance of deep red color and then lyophilized to obtain the dry sample. The hydrodynamic diameter of the Au-NPs were obtained by dynamic light scattering method (Photon Correlation Spectroscopy) and was found to be about 22 nm. The magnetic property of all the samples were measured using MPMS-7 (Quantum Design).

III. RESULTS AND DISCUSSION

In Fig. 3, we show the magnetic hysteresis of the samples taken at 10 and 300 K. We can clearly see that for both the temperatures, the sample B (low Au content) shows a very small enhancement of saturation magnetization whereas the sample C (containing core-shell structure) shows a drastic enhancement in the saturation magnetization. We would

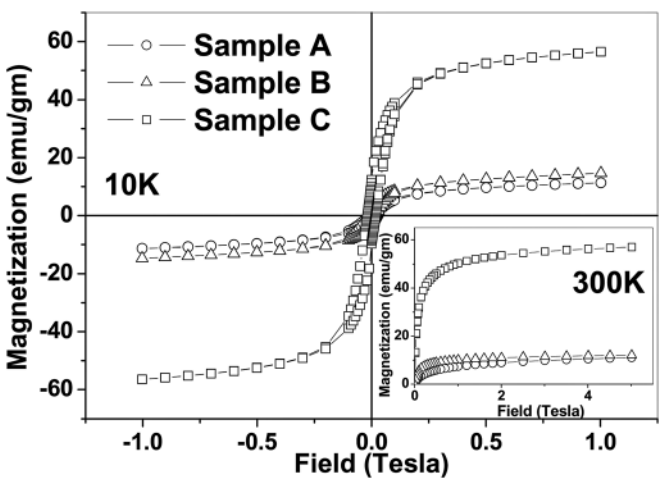

FIG. 3. Magnetization vs H for Sample A (Pure), Sample B (Low-Au), and Sample C (High-Au) taken at 10 K and inset: 300 K.

like to find out the reason for the anomalous increase in magnetization for sample C. As we have emphasized before, the Fe_3O_4 nanoparticles in our sample have a very narrow size distribution as seen from the TEM images. The difference between the three samples is the variation in Au content and their structure. Sample C have core-shell (Fe_3O_4-Au) structure and samples A and B are NPs. The question we would like to pose is: Why for the system containing core-shell structure the magnetization increases drastically? This behavior we believe is new and unexpected. Typically Fe_3O_4 nanoparticle moment density is much lower than that of bulk Fe_3O_4 (Ref. 23) (84 emu/gm). This is due to finite size effects and surface spin canting because of lower coordination number and strain at the surface of the NP.[24] It has been observed that in Au coated Fe_3O_4 nanoparticles the moment reduces further,[11,25] indicating that surface moments might be further disordered due to interaction with Au electrons, leading to the reduced moment. Our system Au-Fe_3O_4 sample C is very different from their core-shell structure because their particle sizes are much smaller than our sample. The sample C has large core-shell particles having large interface between Au and Fe_3O_4. In any case the disordering of canted moments on Fe_3O_4 surfaces due to conduction electrons of Au should still be occurring and hence an increase of net moment is rather surprising. A simple guess would be that Fe_3O_4 is spin polarizing Au very close to the interface. This will increase the net moment as well as increase the effective volume of the magnetic nanoparticles. Spin polarization of non-magnetic metals in contact with ferromagnets was studied extensively experimentally by Hauser[26] and theoretically by Clogston.[27] They found that the spin polarization can at best penetrate a length scale of 1–2 nm in a nonmagnetic metal in contact with a ferromagnet. This is rather small to explain the large change in saturation magnetization coming from an effective volume increase of magnetic nanoparticle due to spin polarization of Au electrons near the interface.

Since spin polarization does not extend to large distances, it cannot explain the continued increase in net moment with increase in Au content. Experimentally magnetic moment of Au near Co/Au interface has been measured from magnetic x-ray circular dichroism[28] to be about 0.062 μ_B per Au atom near the interface. The origin is the spin-orbit splitting of Au surface states (inversion symmetry is lost on the surface), but the moments are far too small (by a factor of 100) to explain our observed increase in moment in Fe_3O_4-Au core-shell system. So we have to look elsewhere to explain this phenomenon and in this paper we present the mechanism to explain our observations.

A set of interesting experimental results on the magnetic properties of some nanostructures has been recently published. Large magnetic moments were detected on the surface layers of thin films of borides and oxides.[13,14] Ferromagnetic hysteresis at room temperature was measured in Au nanoparticles[29] and Au nanoparticles/films with thiol patches on top.[30,31] Spin splitting of surface electronic states was observed in Au(111) (Ref. 36) and Bi.[33] Similar magnetism was detected in Pd nanoparticles also.[34] Usual understanding of magnetism in polymer or thiol stabilized Au NPs is that, there is considerable amount of charge transfer from Au to polymer or thiol, exposing d-holes, which are for some reason polarized to give a net moment. Recently an alternative theoretical attempt was made by Hernando *et al.*[35] to explain magnetic moment in Au with thiol patches on top. Important difference of our system is that here we have an interface between Au and magnetic Fe_3O_4 unlike Au and non-magnetic thiol. As we shall see, this has significant consequences.

We shall assume the existence of a contact potential V and a radial electric field (perpendicular to the interface) $E = -(dV/dr)_{r=\eta}$ at the Au-Fe_3O_4 interface. This will induce a Rashba type spin-orbit interaction, $H_{spin-orbit} = \mu_B/c^2(v \times E) \cdot s = -\alpha\hbar^2 L_z s_z$. Here η is the radius of the interface of any Au particle with the surrounding Fe_3O_4 particles, α is the spin-orbit coupling strength and is proportional to the gradient of the contact potential. Free electrons on the surface of the Au nanoparticles, can be captured in large atomic like bound orbitals of radius η at the domain boundary potential step. With the spin component of the bound Au electron along the z axis being s_z, the Hamiltonian (in the absence of external magnetic field), for these bound electrons can be written down as

$$H = \frac{\hbar^2 L_z^2}{2m\eta^2} - \alpha\hbar^2 L_z s_z + \lambda s \cdot \sum_{i\in\text{interface}} S_i. \qquad (1)$$

λ is the exchange (antiferromagnetic[27]) coupling strength of the Au electron having spin s and i being site index of the Fe moments along the interface having a spin S_i. The first term is the kinetic energy of the electrons near the interface with angular momentum L. The second term is the spin-orbit interaction induced by the interface potential gradient. The third term is the contact exchange interaction of these electrons near the interface with the Fe moments on the surface of the Fe_3O_4 nanoparticles. We have neglected the Zeeman term proportional to external magnetic field, because it is very small (see the estimate later in the text).

We take the average Au nanoparticle radius as $\eta = 4$ nm (the average size (diameter) of the Au NPs is 7–10 nm as seen from TEM measurements). For the spin-orbit coupling we take $\alpha\hbar^2 = 0.4$ eV. This value is large and close to the atomic spin-orbit coupling of the 6p states of Au atoms of 0.47 eV.[32] Experimentally observed spin splitting of the surface states of pure Au(111) surfaces[36] could be explained by assuming $\alpha\hbar^2 = 0.4$ eV. Theoretically it was shown[37] with a simple tight binding model for the surface states, that indeed the spin-orbit coupling for the surface states can be as large as the atomic spin-orbit coupling. It was also pointed out[37] that the magnitude of the surface potential (closely related to the work function of Au), as well as other potential steps on the surface, can further increase the effective spin-orbit coupling of the surface states. In our case with interface with oxide particles, we believe that 0.4 eV for the spin-orbit coupling interaction is an underestimate.

We also take $\lambda = 0.05$ eV (typical values of contact exchange interaction)[27] for illustrative purposes and write the Hamiltonian as

$$H = \frac{\hbar^2 L_z^2}{2m\eta^2} - \alpha\hbar^2 L_z s_z + \lambda s_z \langle M_z \rangle + \lambda \sum_{i\in\text{interface}} \frac{1}{2}(S_i^+ s^- + S_i^- s^+), \qquad (2)$$

where $\langle M_z \rangle = \sum_{i\in\text{interface}} \langle S_{i,z} \rangle$ is the net average z component moment of the surface Fe atoms. The last term is the transverse part of the contact exchange interaction that gives rise to spin flip scattering between the boundary Fe moments and the Au electrons (both bound and free electrons). Forgetting the last term for the time being, we find that when $M_z = 0$ the energy is negative for $L_z = 1$ to 93, i.e, one could have 93 electrons filling such bound orbitals all with same s_z. In Fig. 4, we have plotted the energy versus L_z values for different values of M_z. We can see that for $M_z > 190$ there are no bound states (negative energy) at all for the chosen values of parameters. In other words, if the z component of the boundary spins add up to large values then it is not possible to have bound Au electrons along the interface with large orbital angular momenta. On the other hand when average $M_z = 0$ like in Au-thiol (nonmagnetic) interface, it is

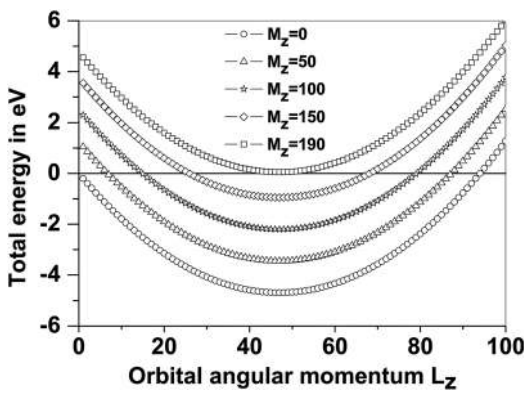

FIG. 4. Total energy in eV vs angular momentum L_z of an electron near the interface.

possible to have large number of bound states occupied with electrons (having L_z values from 1 to large values, and same s_z to minimize exchange part of the coulomb correlation energy) near the interface, giving a large net moment. Interestingly it was found by Crespo *et al.*[38] that with addition of Fe impurity the thiol capped Au nanoparticle magnetism disappears very quickly. This curious observation is easily understandable from the above theoretical discussion of ours.

The spin flip scattering [the last term in Eq. (2)] by the free as well as bound Au electrons with the boundary Fe moments, on the other hand try to randomize the Fe moments giving rise to lesser M_z value. Thus, samples with larger Au concentration will have larger concentration of free electrons, and hence reduces the average boundary Fe moments more efficiently compared to sample with lesser Au/free electron concentration. This could be one of the reasons why, we find larger moment in samples with larger amount of Au interface. It has to be emphasized that the dominant reasons for expecting low values for M_z, which is essential for survival of these interface states is surface spin canting due to lower coordination number and strain or structural deformation at the surface. Moreover, at lower temperatures the surface spins are often in a frozen spin glass state.

Though many groups[10,11,25] have worked with Fe_3O_4-Au nanoparticle composites, to our knowledge, there has been no report so far on such large enhancement of net magnetization of the composite. There could be several reasons for that. (1) If the value of effective η is very small for very small sized Au nanoparticles then the interfaces deviates from a plane too much. Hence, in thiol coated Au nanoparticle system the moment/Au atom is very large in thin films compared to small nanoparticles.[30] (2) On the other hand if the Au particles are large, then the core diamagnetism of Au electrons may cancel out the large orbital moments at the interface. Thus, there seems to be an optimum size of the Au particle which will show maximum magnetization, beyond which the diamagnetic term will dominate. In our case the base material (Fe_3O_4) itself is magnetic and Au-diamagnetism is very small compared to the magnetic base material.

When $M_z = 0$, the net energy of an electron at the interface with orbital angular momentum L_z and spin S_z is

$$E = \frac{\hbar^2 L_z^2}{2m\eta^2} - \alpha\hbar^2 L_z S_z - \mu_B H \cdot (L_z + g_s S_z), \tag{3}$$

where $g_s = 2$. We see that the energy remains negative (bound state) up to, $L_z^{Max} = \alpha m \eta^2$ (taking $S_z = 1/2$). Taking the values of the parameters as in Eq. 2, we find $L_z^{Max} = 93$. If we put electrons in orbitals with $L_z = 1, 2, 3....N$ all with $S_z = 1/2$ then net moment M is $[\frac{N(N+1)}{2} + N]\mu_B$. Putting $N = 93$ we get $M = 4464\mu_B$. The net energy of N electrons is given by

$$\begin{aligned} E_N &= \frac{\hbar^2}{2m\eta^2}\sum_{n=1}^{N} n^2 - \frac{\alpha\hbar^2}{2}\sum_{n=1}^{N} n - H \times 4464\mu_B \\ &= \frac{\hbar^2}{2m\eta^2}\frac{N(N+1)(2N+1)}{6} - \frac{\alpha\hbar^2}{2}\frac{N(N+1)}{2} \\ &\quad - H \times 4464\mu_B \end{aligned} \tag{4}$$

with $N = 93$ the contribution from the first two terms is $E_N = -295.89$ eV. The contribution of the last term (Zeeman) is only -1.39 eV for a magnetic field of 5 T and hence can be neglected [and this is why we have not considered this term in Eq. (1)].

We have neglected the coulomb interaction between these electrons so far. Let us consider it now. In atomic orbitals of extent $r = 1-2\times10^{-8}$ cm, the coulomb correlation energy between two electrons in two different orbitals is about $1-2$ eV; we take 2 eV to have an upper limit on the coulomb repulsion energy. So the average electron-electron interaction energy in orbitals of size $\eta = 40 \times 10^{-8}$ cm is about $\frac{2}{40} = 0.05$ eV. Total coulomb interaction energy of N electrons is about $E_{coulomb} = +\frac{N(N-1)}{2} \times 0.05 = +213.9$ eV. So we see that the total energy $E_{tot} = E_N + E_{coulomb}$ is still negative for $N = 93$, indicating that it is possible to have many electrons at the interface.

Now we are ready to make an estimate about how much moment one should expect in samples B and C. From the measured high field magnetization we find that for pure iron oxide particles (sample A), the magnetization is 12 emu/gm. Taking a density of 5 gm/cm^3, we have 6×10^{21} μ_B/cm^3 moment for pure Fe_3O_4.

The high field magnetization of the sample B is about 14 emu/gm or about 7×10^{21} μ_B/cm^3, assuming the same density. With 10.82% Au in sample B, the net moment/cm^3 coming from 89.18% Fe_3O_4 and orbital moment from the interfaces of 10.82% Au is about

$$\begin{aligned} M_{Total} &= 0.8918 \times 6 \times 10^{21}\mu_B + \frac{0.1082}{\frac{4\pi}{3} \times \eta^3} \times 4464\mu_B \\ &= 7.154 \times 10^{21}\mu_B \end{aligned} \tag{5}$$

This is close to the high field magnetization $7 \times 10^{21}\mu_B$ of sample B. Now assuming 28.7% Au in sample C, we find that the expected net magnetization/cm^3 should be about 9.06×10^{21} μ_B/cm^3. The measured high field magnetization of sample C, on the other hand is about 58 emu/gm, or 29×10^{21} μ_B/cm^3, which is considerably higher than the calculated value. This large value of the magnetization can be accounted by considering a very large interfacial area of the large core-shell structured Fe_3O_4-Au particles in sample C. As we have mentioned before, we see a few large sized core-shell type of particles of diameter 200 nm range. Since $L_z^{Max} \propto \eta^2$, the net orbital magnetic moment per Au NP $M = \frac{L_z^{Max}(L_z^{Max}+1)}{2} \propto (L_z^{Max})^2 \propto \eta^4$. Thus the large particles (core-shell particles) with interface radius about 50 nm, i.e., the radius of the core Fe_3O_4 particle will have orbital magnetic moments about 10^4 times larger than the smaller NPs. In Fig. 5, we have plotted the magnetic moment at the interface of a Au-Fe_3O_4 NP versus the interface radius of the NP, showing the steep increase of the moment with increase in size of the interface.

The difference between the calculated and the observed value of the moment for sample C is around 20×10^{21} μ_B. This additional moment can be obtained by simply considering just 2% of the total particles to be core-shell structure with $\eta = 50$ nm and M $= 10^4$ times the moment of the

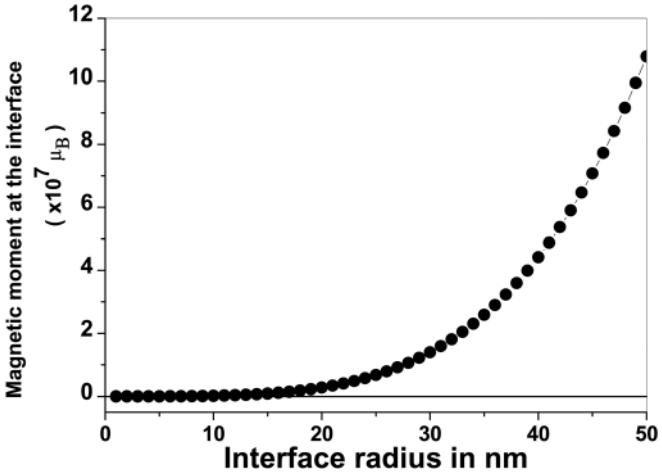

FIG. 5. Net magnetic moment (orbital + spin) of the bound electrons near the interface (in μ_B) vs the radius of the interface (in nm).

smaller NP as mentioned above. Hence we infer that the huge increase in the magnetic moment of Fe_3O_4-Au composites in sample C is coming from mainly the large size core-shell NPs present.

However, one may be concerned regarding the influence of the ratio of Fe(II) to Fe(III) at Fe_3O_4-Au interface on modifying the magnetic property of our system as pointed out in Fe_3O_4 system.[39,40] Of course, there will be a distribution of Fe(II) having S = 2.0 and Fe(III) having S = 2.5 on the surface of the particle unlike in the bulk having one-third of Fe(II) and two-third of Fe(III). But, due to presence of spin flip scattering by the free and bound Au electrons with the boundary Fe moments, lower coordination number, structural deformation at the interface, and some more factors which we have mentioned earlier will reduce drastically the M_z value. In Fig. 4, we show how by simply randomizing the surface moment one get large orbital angular momentum L_z leading to enhancement of magnetization of the system as discussed above.

If the magnetism in Au NPs arise due to the interfacial contact potential, then this should also be seen in a system containing interface of Au with nonmagnetic material. We have used Au-NPs coated with citrate to verify magnetism arising due to the interfacial effect. Figure 6 shows the M versus H curves of the Au-citrate NPs taken at three different temperatures (T = 5, 100, and 300 K) up to 7 T magnetic field. We observe the following. (1) The saturation magnetization at 5 K (occurring beyond 7 T) is an order of magnitude more than that at 100 and 300 K. (2) The magnetization at 100 and 300 K shows a crossover from a positive magnetization to a negative magnetization (diamagnetic state) at ~6 and ~1 T, respectively. (3) Faint hysteresis is observed at 5 K.

With an average Au NP radius of 11 nm, and the saturation magnetic moment at the lowest temperatures $T = 5$ K, and a field of 7 T, we estimate the average magnetic moment/Au NP to be about 1115 μ_B. If L_m is the maximum L_z value of any bound state electron, then the net moment of that particular Au NP is about

$$M = \frac{L_m(L_m+1)}{2} + L_m \approx \frac{L_m^2}{2}, \qquad (6)$$

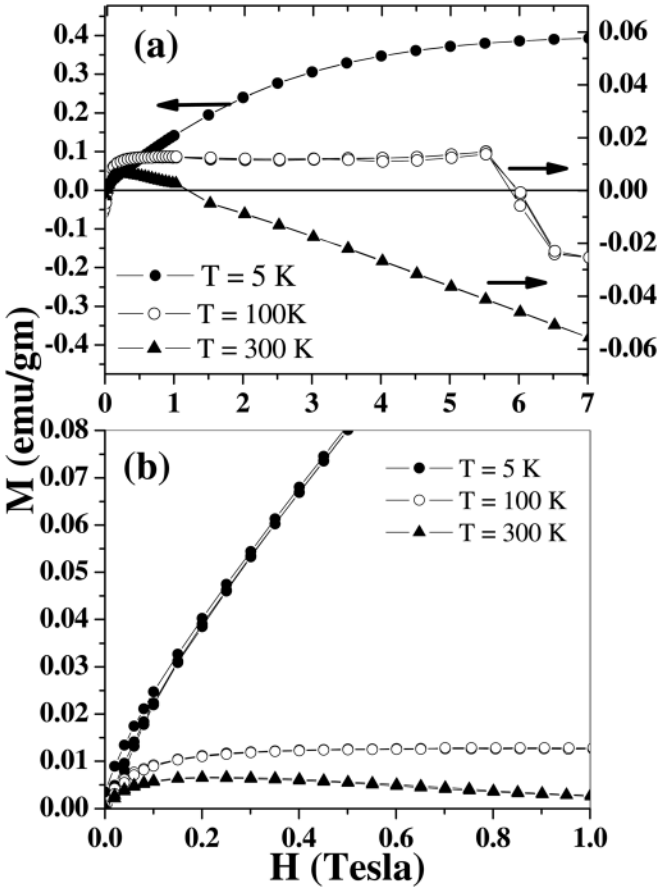

FIG. 6. (a) Magnetization vs H for the Au-citrate sample taken at 5, 100, and 300 K up to a field of (a) 7 T and (b) expanded scale up to 1 T.

so we get $\frac{L_m^2}{2} = 1115\ \mu_B$ or $L_m = 47\ \mu_B$. Since, also, $L_m = \alpha m \eta^2$, we find that the necessary spin-orbit coupling, to get $L_m = 47$ is about = 56.76 meV.

Remembering that for Fe_3O_4-Au composite we have taken $\alpha\hbar^2 = 0.4$ eV, the value for Au-citrate interface is less than 0.4 eV by a factor of 7. This is reasonable, as can be seen from the following arguments. We have assumed that, in an interface between metal/insulator there is charge transfer from the metal to the insulator. But a good upper bound of the amount of charge transfer, will be when the field created at the interface due the charge transfer is nearly equal to the dielectric breakdown field of the insulator. The dielectric breakdown field of organic polymers is about 50–900 KV/cm. Thin films of metal oxides dielectric breakdown field depends on defect concentration as well as thickness. For SiO_2 for example, this field varies from 1–10 MV/cm[41,42] and for organic thin films like polyethylenes, benzene, this field is about 0.5 MV/cm.[43] It is likely that transition material oxide like Fe_3O_4 will presumably have a breakdown field of the same order of magnitude as SiO_2. Since spin-orbit coupling is proportional to this field, a factor of 7 seems reasonable.

Using the arguments given earlier, we can explain the crossover from the magnetic to a diamagnetic state observed in the magnetization at higher temperatures. Let us assume that the total magnetization observed in these particles is due to the addition of the diamagnetic and the interfacial ferromagnetic contributions. The interfacial moment contribution

at 5 K is very large compared to that at 100 and 300 K because we observe the saturation magnetization to be much smaller at 100 and 300 K (observation (1) above). Since diamagnetic contribution is independent of temperature, at higher temperatures, the diamagnetic contribution can overcome the low interfacial magnetic contribution at a lower field (observation (2) above). Hence we see a crossover from a low (positive) saturation magnetization to a (negative) diamagnetic behavior. Assuming a paramagnetic scaling of the orbital moment ($M \propto H/T$), and assuming the bulk diamagnetic susceptibilty (temperature independent) of Au to be about $\chi_{dia} = 2.8 \times 10^{-6}$ emu/(cc Oe), we find the field at which the total magnetic moment should do the zero crossing for temperatures, T = 100 K and T = 300 K should be about H = 4 T and H = 0.6 T. Experimentally, these fields are 5.5 and 1 T, respectively. Note: The crossover from a positive to a negative value in the magnetization is an interesting observation. Hence, this observation clearly indicates that the interfacial effect is the most likely phenomena for the observed magnetism in Au NPs.

IV. CONCLUSION

In the present investigation, we have observed that it is possible to increase the net magnetic moment of Fe_3O_4 NPs by coating with Au NPs on an aggregate of Fe_3O_4 NPs creating a core-shell structure. The chemical potential gradient at the interface of the Fe_3O_4-Au is enough to trap the conduction electrons from the Au particle and induce a large orbital moment at the interface. Thus, the enhanced magnetic moment is argued to come from metallic electrons at the Au-Fe_3O_4 interface and predominantly orbital in origin. We have also found that to have very large increase in net magnetic moments, it is necessary to have core-shell type particles with large interface. We have done quantitative estimates of such induced magnetic moments and compared with our experimentally measured values. The agreement between theory and experiment is reasonably good. We have also shown that this interfacial effect is the most likely phenomena for the observation of magnetism in Au-NPs by showing magnetism in citrate coated gold Au-NPs. The observation of sudden transition of positive magnetization to negative diamagnetic magnetization as a function of magnetic field could be explained by the destruction of the interfacial magnetic moment by the diamagnetic contribution.

ACKNOWLEDGMENTS

The authors thank the TEM facility at Institute of Physics, Bhubaneswar for the TEM measurements.

[1]S. Bedanta and W. Kleemann, J. Phys. D. Appl. Phys. **42**, 013001 (2009).
[2]J. L. Dormann, D. Fiorani, and E. Tronc, Adv. Chem. Phys. **98**, 283 (1997).
[3]J. L. Dormann, L. Bessais, and D. Fiorani, J. Phys. C: Solid State Phys. **21**, 2015 (1988).
[4]P. P. Freitas and H. A. Ferreira, *Handbook of Magnetism and Magnetic Materials*, edited by H. Kronmuller and S. P. S. Parkin (Wiley, New York, 2007), Vol. 4, p. 2507.
[5]V. L. Vaidhianathan and B. Singh, Nature **128**, 302 (1931), and references therein.
[6]S. Banerjee, M. Mandal, N. Gayathri, and M. Sardar, Appl. Phys. Lett. **91**, 182501 (2007).
[7]L. Wang *et al.*, J. Mater. Chem, **18**, 2629 (2008).
[8]H. Kim *et al.*, J. Am. Chem. Soc. **127**, 544 (2005).
[9]J. W. Yoo *et al.*, J. Phys. Chem. A **106**, 2049 (2002).
[10]J. Lin *et al.*, J. Solid State. Chem. **159**, 26 (2001).
[11]L. Wang, J. Luo, Q. Fan, M. Suzuki, I. S. Susuki, M. H. Engelhard, Y. Lin, N. Kim, J. Q. Wang, and C.-J. Zhong, J. Phys. Chem. B **109**, 21593 (2005).
[12]P. Esquinazi, D. Spemann, R. Hhne, A. Setzer, K.-H. Han, and T. Butz, Phys. Rev. Lett. **91**, 227201 (2003); K. Kusakabe and M. Maruyama, Phys. Rev. B **67**, 092406 (2003); P. O. Lehtinen, A. S. Foster, Y. Ma, A. V. Krasheninnikov, and R. M. Nieminen, Phys. Rev. Lett. **93**, 187202 (2004).
[13]M. Venkatesan, C. B. Fitzgerald, and J. M. D. Coey, Nature **430**, 630 (2004).
[14]L. S. Dorneles, M. Venkatesan, M. Moliner, J. G. Lunney, and J. M. D. Coey, Appl. Phys. Lett. **85**, 6377 (2004).
[15]S. Banerjee and D. Bhattacharya, Comp. Mat. Sci. **44**, 41 (2008).
[16]H. Hori *et al.*, Phys. Lett. A **263**, 406 (1999); H. Hori *et al.*, Phys. Rev. B **69**, 174411(2004); Y. Yamamoto *et al.*, Phys. Rev. Lett. **93**, 116801 (2004).
[17]P. Zhang and T. K. Sham, Phys. Rev. Lett. **90**, 245502 (2003); P. Crespo *et al.*, Phys. Rev. Lett. **93**, 087204 (2003).
[18]J. S. Gartaonandia *et al.*, J. Appl. Phys. **105**, 07A907 (2009); Nano Letters **8**, 661 (2008).
[19]J. de la Venta *et al.*, J. Nanosci. Nanotech. **9**, 6434 (2009).
[20]T. Taniyama, E. Ohta, and T. Sato, Euro. Phys. Lett. **38**, 195 (1997); W. H. Lai *et al.*, Phys. Rev. Lett. **89**, 135504 (2002); T. Shinohara, T. Sato, and T. Taniyama, Phys. Rev. Lett. **91**, 197201 (2003).
[21]J. J. Shen, W. B. Mi, Z. Q. Li, P. Wu, E. Y. Jiang, and H. L. Bai, J. Phys. D: Appl. Phys. **39**, 3726 (2006).
[22]J. Polte, R. Erler, A. F. Thunemann, S. Sokolov, T. T. Ahner, K. Rademann, F. Emmerling, and R. Kraehnert, ACS-Nano **4** 1076 (2010).
[23]J. Wang, J. Sun, Q. Sun, and Q. Chen, Mat. Res. Bull. **38**, 1113 (2003).
[24]R. H. Kodama, A. E. Berkowitz, E. J. McNiff, Jr., and S. Foner, Phys. Rev. Lett. **77**, 394 (1996); B. Martinez, X. Obrados, L. Balcells, A. Rpuanet, and C. Monty, Phys. Rev. Lett. **80**, 181 (1998).
[25]S. Pal, M. Morales, P. Mukherjee, and H. Srikanth, J. Appl. Phys. **105**, 07B504 (2009).
[26]J. J. Hauser, Phys. Rev. **187**, 580 (1969).
[27]A. M. Clogston, Phys. Rev. Lett. **19**, 583 (1967).
[28]F. Wilhelm, M. Angelakeris, N. Jaouen, P. Poulopoulos, E. T. Papaioannou, C. Mueller, P. Fumagalli, A. Rogalev, and N. K. Flevaris, Phys. Rev. B 69, 220404(R) (2004).
[29]Y. Yamamoto, T. Miura, M. Suzuki, N. Kawamura, H. Miyagawa, T. Nakamura, K. Kobayashi, T. Teranishi, and H. Hori, Phys. Rev. Lett. **93**, 116801 (2004).
[30]P. Crespo, R. Litrán, T. C. Rojas, M. Multigner, J. M. de la Fuente, J. C. Sánchez-López, M. A. García, A. Hernando, S. Penadés, and A. Fernández, Phys. Rev. Lett. **93**, 087204 (2004).
[31]L. Carmeli, G. Leitus, R. Naaman, S. Reich, and Z. Vager, J. Chem. Phys. **118**, 10372 (2003).
[32]C. E. Moore, Atomic Energy Levels (National Bureau of Standards, Washington DC, 1949).
[33]Y. M. Koroteev, G. Bihlmayer, J. E. Gayone, E. V. Chulkov, S. Blügel, P. M. Echenique, and P. Hofmann, Phys. Rev. Lett. **93**, 046403 (2004).
[34]B. Sampedro, P. Crespo, A. Hernando, R. Litrán, J. C. Sánchez López, C. López Cartes, A. Fernandez, J. Ramírez, J. González Calbet, and M. Vallet, Phys. Rev. Lett. **91**, 237203 (2003); T. Shinohara, T. Sato, and T. Taniyama, Phys. Rev. Lett. **91**, 197201 (2003).
[35]A. Hernando, P. Crespo, and M. A. García, Phys. Rev. Lett. **96**, 057206 (2006).
[36]S. Lashell, B. A. Mcdougall, and E. Jensen, Phys. Rev. Lett. **77**, 3419 (1996).
[37]L. Petersen and P. Hedegard, Surf. Sci. **459**, 49 (2000).
[38]P. Crespo *et al.*, Phys. Rev. Lett. **97**, 177203 (2006).
[39]X.-L. Tang, H.-W. Zhang, H. Su, Z.-Y. Zhong, and Y.-L. Jing, J. Vac. Sci. Technol. A **25** 1489 (2007).
[40]W. B. Mi, E. Y. Jiang, and H. L. Bai, J. Phys. D: Appl. Phys. **42** 105007 (2009).
[41]M. Badila *et al.*, Thin Solid Films **192**, 1 (1990).
[42]S. K. Rha *et al.*, Curr. Appl. Phys. **9**, 551 (2009).
[43]D. R. Lide, *Handbook of Chemistry and Physics* (CRC Press, Taylor and Francis, New York, 2007-2008).